Synbindin downregulation participates in slit diaphragm dysfunction

Veniamin Ivanov, Yoshiyasu Fukusumi, Ying Zhang, Hidenori Yasuda, Meiko Kitazawa & Hiroshi Kawachi

Department of Cell Biology, Kidney Research Center, Niigata University Graduate School of Medical and Dental Sciences

Short Title: Synbindin in podocytes

Correspondence to;

Hiroshi Kawachi, MD, PhD.

Department of Cell Biology, Kidney Research Center, Niigata University Graduate School of Medical and Dental Sciences, Niigata, 951-8510, Japan.

E-mail : kawachi@med.niigata-u.ac.jp.

Phone : +81-25-227-2159, Fax : +81-25-227-0770

Number of Tables: 0
Number of Figures: 4
Number of Supplementary Material: 2
Word count: 4321 (Abstract, Introduction, Materials & Method, Results Discussion, Acknowledgement, Reference)

Key Words: synbindin, podocyte, slit diaphragm, nephrin, SV2B

Abstract

Introduction: Synbindin, originally identified as a neuronal cytoplasmic molecule, was found in glomeruli. cDNA subtractive hybridization technique showed the mRNA expression of synbindin in glomeruli was down-regulated in puromycin aminonucleoside (PAN) nephropathy, a mimic of minimal-change nephrotic syndrome.

Methods: The expression of synbindin in podocyte was analyzed in normal rats and two types of rat nephrotic models, anti-nephrin antibody (ANA)-induced nephropathy a pure slit diaphragm injury model and PAN nephropathy by immunohistochemical analysis and RT-PCR techniques. To elucidate the function of synbindin, a gene silencing study with human cultured podocytes was performed.

Results: Synbindin was mainly expressed at slit diaphragm area of glomerular epithelial cells (podocytes). In both nephrotic models, decreased mRNA expression and the altered staining of synbindin were already detected at the early phase when proteinuria and the altered staining of nephrin, a key molecule of slit diaphragm, were not detected yet. Synbindin staining was clearly reduced when severe proteinuria was observed. When the cultured podocytes were treated with siRNA for synbindin, the cell changed to be round-shape, and filamentous actin structure was clearly altered. The expression of ephrin-B1, a transmembrane protein at slit diaphragm, was clearly lowered, and synaptic vesicle-associated protein 2B (SV2B) was upregulated in the synbindin knockdown cells.

Conclusion: Synbindin participates in maintaining foot processes and slit diaphragm as a downstream molecule of SV2B-mediated vesicle transport. Synbindin downregulation participates in slit diaphragm dysfunction. Synbindin can be an early marker to detect podocyte injury.

Introduction

Glomerular visceral epithelial cells (podocytes) are highly differentiated cells characterized by multiple interdigitating foot processes. The basal side of foot processes is connected to the glomerular basement membrane (GBM) by α3β1-integrin, and neighboring foot processes are connected via slit diaphragm. Effacement of foot processes and detachment of foot processes from GBM are important and common morphological alterations of podocyte injury in nephrotic syndrome. It is now accepted that the dysfunction of the slit diaphragm is involved in the development of proteinuria in several glomerular diseases [1]. In the past two decades, some functional molecules of podocytes such as nephrin [2], podocin [3], NEPH1[4] have been identified. However, the precise molecular composition involved in the interaction between foot processes and GBM and the molecular structure of the slit diaphragm are not well understood yet.

To identify novel functional molecules of the podocyte, we performed cDNA subtractive hybridization of glomerular cDNA from normal rats and rats with puromycin aminonucleoside (PAN)-induced nephropathy, which is widely used as an experimental model of human minimal-change nephrotic syndrome (MCNS) [5]. It is conceivable that the molecules downregulated before the onset of proteinuria might be functional molecules and that the downregulation is involved in the development of proteinuria. Thus, we intended to purify the molecules whose expressions were decreased at 24 h after the PAN injection.

In a series of studies, we identified several genes downregulated at 24 h of PAN nephropathy. We reported that synaptic vesicle protein 2B, (SV2B), ephrin-B1, and some other molecules play critical roles in maintaining specialized functions of podocytes [6,7,8,9,10]. In the present study, we focused on synbindin, which was identified as a neuronal cytoplasmic molecule interacting with syndecan-2 [11]. Synbindin is homologous to several PDZ domain proteins and binds to the PDZ-binding domain of syndecan-2 [11]. Fan, et al. revealed the crystal structure of human synbindin [12]. However, studies on synbindin are still very few. Synbindin was reported to be necessary for the syndecan-2-mediated spine formation in nerve cells [11]. It has been pointed out that neurons and podocytes have common characteristics [8,13]. Both are terminally differentiated cells and have similar shapes characterized by unique processes. The properties of synbindin prompted us to speculate that synbindin plays an essential role in podocytes.

In the present study, we demonstrated that synbindin is mainly expressed at the slit diaphragm area of glomerular epithelial cells (podocytes). The expression of synbindin was lowered not only in PAN nephropathy but also in anti-nephrin antibody

(ANA)-induced nephropathy, a pure slit diaphragm dysfunction model. The expression of synbindin decreases rapidly just after disease induction of the nephrotic models, which suggests that synbindin participates in the initiation event of podocyte injury and that synbindin can be an early marker to detect podocyte injury,

Materials and Methods

Animal Experiments

All animal experiments conformed to the NIH Guide for the Care and Use of Laboratory Animals [14] and were approved by the Animal Committee at Niigata University, Japan, permit numbers SA00710. Specific pathogen-free female Wistar rats purchased from Charles River (Atsugi, Japan) were used. For the analysis of developmental expression, neonatal Wistar rats were used. For preparing one set of PAN nephropathy [6], a total of 12 rats were used. Three rats were sacrificed before injection, and 9 rats were injected with 10 mg/100g BW of PAN, and three rats at each time point were sacrificed at 1 h, 24 h, and 10 days after the injection. For preparing a set of ANA-induced nephropathy [15-17], a total of 12 rats were used. Three rats were sacrificed before injection, and 9 rats were injected with 15 mg/rat of anti-nephrin antibody [15], and three rats at each time point were sacrificed at 1 h, 24 h, and 5 days after the injection. The urine protein concentration was measured by colorimetric assay with a Protein Assay Reagent (Bio-Rad, Hercules, CA) using BSA as a standard. The average value of the proteinuria is as follows: PAN nephropathy, 24 h; 4.5 mg/day, day 10; 238.7 mg/day, ANA nephropathy: 24 h; 46.6 mg/day, day 5; 215.8 mg/day. Three sets of each model were prepared for the analysis of the mRNA expression of glomeruli.

Immunohistochemical analysis

Immunohistochemical studies were performed basically according to the method previously reported [7,9,18,19,20,21]. The primary antibodies were used as follows: Anti-synbindin antibody was prepared in rabbits immunized with a peptide of 16 amino acids of rat synbindin sequence CIDSLLRKIYEIYSDF. Two rabbits were immunized with 1.0 mg of peptide conjugated with the carrier protein KLH and boosted twice with 0.5 mg of antigen. The rabbits were bled 2 weeks after the last immunization. All primary and secondary antibodies used in this study were summarized in Supplemental Table 1. The immunofluorescence staining of synbindin in glomeruli was semi-quantified basically according to the method previously reported [9].

Real-Time RT-PCR

Real-time RT-PCR analyses were performed according to the method described previously [18]. The glomeruli isolated from pooled kidneys of each set of the models and the cultured podocytes were used for real-time RT-PCR analysis. Ct values of the gene targets were normalized to glyceraldehyde-3-phosphate dehydrogenase (GAPDH). Fold change in expression of target genes compared with the normal rat or Scramble SiRNA was calculated using the 2-ΔΔCT method with GAPDH. The data are shown as ratios relative to control findings and expressed as mean ± SEM of three independent experiments. Primers used in this study were shown in Supplemental Table 2.

Human Podocyte Cell Culture

Human immortalized podocytes were kindly provided by Prof. Moin Saleem (Children's Renal Unit and Academic Renal Unit, University of Bristol, Southmead Hospital, Bristol, UK) and were maintained basically as previously described.[22]

RNA Silencing Analysis

The siRNA targeting synbindin and negative control siRNA were purchased from Thermo Fisher Scientific (Catalog #1299001). Cells were harvested 96 hours after siRNA treatment for real-time RT-PCR analyses and immunofluorescence. Actin staining of the cells was evaluated as score 1-4 as previously described. [9,23]. Actin alteration score was made as follows. Score 0: cell showed normal F-actin staining pattern. Score 1: Staining showed mild alteration of F-actin staining. Score 2: Severe alteration of F-actin staining with no recognition of normal staining. The immunofluorescence intensity was assigned to each cell, and 30 cells of each image were analyzed. For detecting actin fiber, Rhodamine-Phalloidin (Cytoskeleton Inc. Denver, CO) was used.

Statistical analysis

Statistical significance was evaluated using the paired and unpaired t-test or u-test. Values were expressed as the mean ± SEM. Differences at $p < 0.05$ were considered significant. Data were analyzed using Graphpad Prism 5.0 software (Graphpad Software, San Diego, CA).

Results_

Synbindin is expressed in the glomerular podocyte.

Synbindin was dominantly expressed in glomeruli in the kidney section along the capillary loop as a discontinuous dot-like pattern (Fig. 1a). Synbindin staining was apart from endothelial cell marker RECA1 and mesangial cell marker Thy1.1. Major parts of synbindin were colocalized with slit diaphragm markers nephrin and ephrin-B1. A small portion of synbindin was colocalized with podocalyxin, an apical surface marker. No colocalization with basal area marker α3-integrin was detected (Fig. 1b).

Synbindin appears in presumptive podocytes together with nephrin.

To investigate the developmental expression of synbindin, neonatal rat kidney sections were used. At the early S-shaped body stage, synbindin was not detected yet. Synbindin appeared together with nephrin at the late S-shaped body stage (Fig. 1c). The synbindin staining became to be clear with podocyte maturation. The synbindin expression in developing podocytes was generally colocalized with nephrin.

Synbindin staining is clearly altered in nephrotic models.

Next, the immunostaining of synbindin in podocytes was analyzed with dual-labeling immunofluorescence with nephrin in two nephrotic models: ANA and PAN nephropathies. The expression was analyzed at the acute phase (1 and 24 h after disease induction) and at the peak of proteinuria (day 5 in ANA-nephropathy and day 10 in PAN-nephropathy). In both models, a decrease of synbindin staining was already detected at 1h, when a reduction of nephrin staining was not clearly detected yet (Fig. 2). Synbindin staining was clearly reduced when severe proteinuria was observed in both models. The alteration of synbindin staining was more evident in ANA nephropathy. The remaining synbindin and nephrin were clearly dissociated in ANA nephropathy. (Fig. 2a arrows). In PAN nephropathy, nephrin remained was colocalized with synbindin.

mRNA expressions of synbindin and synbindin-related molecules are decreased in nephrotic models

Kinetics of mRNA expressions of synbindin and its related molecules in glomeruli of the nephrotic models were analyzed by real-time RT-PCT techniques. The average values of the ratio to normal of three sets were shown in Fig. 3. Glomerular synbindin was clearly downregulated at 1h of ANA nephropathy (16.37% ± 3.38%) and PAN nephropathy (24.7% ± 6.77%). Synbindin mRNA level remains downregulated at the

peak of proteinuria in ANA (25.24% ± 14.88%) and PAN nephropathy (32.4% ± 11.81%).

Next, mRNA expressions of a synbindin-binding protein, syndecan-2, and another proteoglycan family protein, syndecan-4 were analyzed. mRNA expressions of syndecan-2 and syndecan-4 were decreased in both models in the basically same kinetic pattern as synbindin. Next, mRNA expression of CASK was analyzed since CASK is a PDZ molecule interacting with syndecan-2 and syndecan-4. mRNA expressions of CASK declined similarly to synbindin and syndecans.

Synbindin downregulation results in cytoskeletal alteration in cultured podocytes

Next, to elucidate the function of synbindin in podocytes, a gene silencing study with siRNA for synbindin with cultured podocytes was performed. Synbindin downregulation was confirmed by real-time RT-PCR (15.54% ± 5.52%) and immunofluorescence staining (Fig. 4a). The cell shape of the synbindin siRNA-treated cell changed to a round shape, and the ratio of podocytes with the process was clearly lesser in synbindin siRNA-treated cells than that in scramble siRNA-treated cells (50.55% ± 2.18% vs. 36.67% ± 2.11%, $p < 0.01$). The alteration of cell shape in synbindin siRNA-treated cells was accompanied by derangement of F-actin structures (Fig 4b).

Ephrin-B1 is downregulated, and SV2B is upregulated in synbindin-deleted cells.

Next, to explore synbindin-associated molecules and to address the possible mechanism of synbindin downregulation-induced podocyte alteration, mRNA expressions of syndecans, podocyte critical molecules such as α3-integrin, podocalyxin and slit diaphragm-associated molecules nephrin and ephrin-B1, and SV2B, a synaptic vesicle-associated molecule expressed in podocyte, were analyzed. Neither altered expression of syndecan-2 nor syndecan-4 were detected. mRNA expression of ephrin-B1 was clearly reduced in synbindin siRNA-treated cells, although no evident alteration of podocyte critical molecules such as α3-integrin, podocalyxin, and nephrin was detected. mRNA expression of SV2B was clearly elevated in synbindin siRNA-treated cells (Fig 4c).

Discussion

To identify the molecules essential in maintaining the specialized function of the podocyte, we performed a cDNA subtraction assay with glomerular cDNA from normal and PAN-induced nephropathy rats, which is a mimic of MCNS, one of the most common diseases showing the nephrotic level of proteinuria. The subtraction assay

showed that synbindin mRNA expression clearly decreased at the early phase of PAN nephropathy, suggesting that synbindin is involved in the initiation of podocyte injury.

The result prompted us to investigate the role of synbindin in podocytes.

Synbindin was identified as a syndecan-2-binding protein in the murine neuron by Ethell *et al.* in 2000 [11]. It was also reported that synbindin plays an important role in spine formation in nerve cells. However, few reports on synbindin have been published to date, and no studies on synbindin in podocytes were reported. Based on the Gen-Bank data of deduced amino-acid sequences of synbindin, rat synbindin has 97.7% and 99.1% identity to that of human and mouse, respectively. It is conceivable that the high conservation of synbindin among species suggests that synbindin plays an essential role in maintaining cell function. It was shown that the amino-acid residues of the PDZ-related domain of synbindin are also highly conserved among species, suggesting that synbindin plays a crucial role as a scaffolding protein interacting with the transmembrane proteins holding a PDZ-binding motif. In this study, to elucidate the physiological and pathological role of synbindin in podocytes, we investigated the expression and localization of synbindin in normal rat and two types of rat nephrotic models. Then, to address the function of synbindin in podocytes, the synbindin deletion study with human cultured podocytes was performed.

First, the expression and localization of synbindin in the normal rat kidney section were analyzed. Synbindin was dominantly expressed in glomeruli in the kidney section. Dual labeling IF study with glomerular cell markers showed synbindin was restrictedly expressed in podocytes in glomeruli. The dual-labeling study with subcellular markers of podocyte showed that major parts of synbindin are colocalized with slit diaphragm markers nephrin and ephrin-B1, and another portion of synbindin was colocalized with podocalyxin, an apical cell surface marker. The staining of synbindin is apart from α3-integrin staining. The observations showed that synbindin is mainly expressed at the slit diaphragm area. The developmental study with neonatal kidney sections showed that synbindin appeared at the late S-shaped body stage together with nephrin. In immature podocytes, synbindin staining was broadly detected, and with maturing the staining of synbindin became to be concentrated to the lateral side together with nephrin. (Fig. 1c). All these observations implied that synbindin is associated with the slit diaphragm.

In this study, we analyzed the kinetics of the expression of synbindin in two nephrotic models, PAN nephropathy and ANA nephropathy. ANA nephropathy is a nephrotic model that resulted from the rearrangement of slit diaphragm molecules

caused by stimulation to nephrin [24]. The alterations of synbindin staining were observed not only in PAN nephropathy but also in ANA nephropathy, and the alteration was more evident in ANA nephropathy. The alterations of synbindin expression in both models were detected before the onset of proteinuria, suggesting that the synbindin alteration is not the outcome of proteinuria but has an etiological role in the initiation event of podocyte injury, which leads to proteinuria. Interestingly, the decrease in the intensity of synbindin staining was already detected just after the anti-nephrin antibody injection (1 h after the injection) before the alteration of nephrin staining is not noticed yet. The alterations of synbindin staining become to be more evident on day 5. Dual labeling analysis with nephrin showed that the staining of remaining synbindin was clearly apart from that of nephrin remained in ANA nephropathy. Nephrin remained was colocalized with synbindin in PAN nephropathy, although both synbindin and nephrin decreased. It is conceivable that these findings suggested that synbindin is associated with slit diaphragm and that the alteration of synbindin expression is involved in the initiation phase of slit diaphragm dysfunction. The result indicated that synbindin could be an early marker to detect podocyte injury.

Next, the kinetics of mRNA expression of synbindin and synbindin-related molecules in the nephrotic models was analyzed. We have previously reported that mRNA expressions of slit diaphragm molecules such as nephrin and podocin were downregulated in the nephrotic models [25,26]. In this study, we found mRNA expressions of synbindin and its related molecules were decreased just after disease induction. The kinetics of the alterations in mRNA of synbindin is basically accorded with that of immunostaining. Here we found that synbindin and synbindin-related molecules syndecan-2, syndecan-4, and CASK were altered in similar kinetics to synbindin. The observations implied that the synbindin might be related to these proteoglycans in podocytes, and downregulations of these molecules are involved in the slit diaphragm dysfunction. CASK, a PDZ protein, is understood to function as a scaffolding protein sustaining the transmembrane proteins such as syndecans and is reported to interact with nephrin in podocytes [27,28]. Although the precise interactions between synbindin, proteoglycans, CASK, and slit diaphragm molecules are not clear, the observations implied that synbindin-associated molecules participate in the initiation phase of the slit diaphragm injury.

Next, to investigate the role of synbindin in podocytes, we performed a gene silencing study of siRNA for synbindin with human cultured podocytes. We found that the cells changed to a round shape without processes, and the F-actin structure was deranged in the cells treated with synbindin siRNA. The results implied that synbindin

participates in the formation and/or the maintenance of processes with dense F-actin structure. Then, we analyzed mRNA expressions of the synbindin-related molecules and the slit diaphragm functional molecules in the synbindin-deleted podocytes. Here we found that ephrin-B1, which is one of the critical transmembrane proteins for maintaining the barrier function of slit diaphragm [10], was clearly downregulated in synbindin-deleted cells. We have previously reported that the immunostaining of ephrin-B1 is decreased before the reduction of nephrin staining in ANA nephropathy [7,19]. The finding of ephrin-B1 is similar to that of synbindin observed in this study. These findings suggested that ephrin-B1 is an associated molecule with synbindin, and synbindin may participate in the proper expression of ephrin-B1. Another important finding detected in this analysis is that the expression of SV2B was evidently increased in the synbindin-deleted cells. Although the mechanism of how SV2B is upregulated in the synbindin-deleted cells is not well explained, it is plausible that SV2B upregulated in a negative feedback mechanism compensating the function of synbindin. We have previously reported that some of the critical slit diaphragm components were downregulated in glomeruli of the SV2B KO mice, indicating that SV2B-associated synaptic vesicle-like vesicle participates in the formation and maintenance of slit diaphragm [18]. In the original report on synbindin, Ethell *et al.* reported that synbindin is expressed on intracellular vesicles as well as at the plasma membrane area, and they concluded that synbindin is involved in vesicle transport [11]. Based on the finding obtained in this study with the findings in the previous reports, we propose that synbindin participates in the formation of the interdigitating foot processes and the slit diaphragm connecting neighboring foot processes as a downstream molecule of SV2B.

In conclusion, synbindin is mainly expressed at the slit diaphragm area in podocyte, and the expression of synbindin is rapidly decreased in the nephrotic models when proteinuria and the altered expression of nephrin are not detected yet, which indicating that synbindin participates in the initiation event of podocyte injury and that synbindin could be an early marker to detect podocyte injury.

Acknowledgment;

We thank Mutsumi Kayaba for her excellent technical assistance. A portion of this study was presented at the ASN, St. Louis, Missouri, USA, 2004, and was published in abstract form (J Am Soc Nephrol 15: 239A, 2004).

Statement of Ethics:

All animal experiments conformed to the NIH Guide for the Care and Use of Laboratory Animals [14] and were approved by the Animal Committee at Niigata University, Japan, permit numbers SA00710.

Conflict of interest;

The authors have declared that no conflict of interest exists.

Funding;

This work was supported by Grant-Aids for Scientific Research (19H03673 to H.K., 20K08587 to Y.F. and 19K08720 to Y.Z.) and Grant-Aid for Young Sciences (18K15996 to H.Y.) from Ministry of Education, Culture, Sports, Science and Technology of Japan.

Author Contributions:

V.I. and H.K. designed the experiments; V.I. performed major parts of in vivo and in vitro experiments and wrote the manuscript; Y.Z. and M.K. contributed to the in vivo experiments. Y.F. and H.Y. contributed to the human cultured podocyte study; H.K. conceived and directed the project and wrote the manuscript.

References

1. Kawachi H, Fukusumi Y. New insight into podocyte slit diaphragm, a therapeutic target of proteinuria. Clin Exp Nephrol. 2020 Mar;24 (3):193-204.
2. Kestila M, Lenkkeri U, Mannikko M, Lamerdin J, McCready P, Putaala H, et al. Positionally cloned gene for a novel glomerular protein--nephrin--is mutated in congenital nephrotic syndrome. Mol Cell. 1998 Mar;1 (4):575-582.
3. Boute N, Gribouval O, Roselli S, Benessy F, Lee H, Fuchshuber A, et al. NPHS2, encoding the glomerular protein podocin, is mutated in autosomal recessive steroid-resistant nephrotic syndrome. Nat Genet. 2000 Apr;24 (4):349-354.
4. Donoviel DB, Freed DD, Vogel H, Potter DG, Hawkins E, Barrish JP, et al. Proteinuria and perinatal lethality in mice lacking NEPH1, a novel protein with homology to NEPHRIN. Mol Cell Biol. 2001 Jul;21 (14):4829-4836.
5. Kawachi H, Koike H, Kurihara H, Sakai T, Shimizu F. Cloning of rat homologue of podocin: expression in proteinuric states and in developing glomeruli. J Am Soc Nephrol. 2003 Jan;14 (1):46-56.
6. Miyauchi N, Saito A, Karasawa T, Harita Y, Suzuki K, Koike H, et al. Synaptic vesicle protein 2B is expressed in podocyte, and its expression is altered in proteinuric glomeruli. J Am Soc Nephrol. 2006 Oct;17 (10):2748-2759.
7. Hashimoto T, Karasawa T, Saito A, Miyauchi N, Han GD, Hayasaka K, et al. Ephrin-B1 localizes at the slit diaphragm of the glomerular podocyte. Kidney Int. 2007 Oct;72 (8):954-964.
8. Saito A, Miyauchi N, Hashimoto T, Karasawa T, Han GD, Kayaba M, et al. Neurexin-1, a presynaptic adhesion molecule, localizes at the slit diaphragm of the glomerular podocytes in kidneys. Am J Physiol Regul Integr Comp Physiol. 2011 Feb;300 (2):R340-348.
9. Takamura S, Fukusumi Y, Zhang Y, Narita I, Kawachi H. Partitioning-Defective-6-Ephrin-B1 Interaction Is Regulated by Nephrin-Mediated Signal and Is Crucial in Maintaining Slit Diaphragm of Podocyte. Am J Pathol. 2020 Feb;190 (2):333-346.
10. Fukusumi Y, Yasuda H, Zhang Y, Kawachi H. Nephrin-Ephrin-B1-NHERF2-Ezrin-Actin axis is critical in podocyte injury. Am J Pathol. 2021 Apr;
11. Ethell IM, Hagihara K, Miura Y, Irie F, Yamaguchi Y. Synbindin, A novel syndecan-2-binding protein in neuronal dendritic spines. J Cell Biol. 2000 Oct;151 (1):53-68.

12. Fan S, Feng Y, Wei Z, Xia B, Gong W. Solution structure of synbindin atypical PDZ domain and interaction with syndecan-2. Protein Pept Lett. 2009;16 (2):189-195.
13. Kobayashi N, Mundel P. A role of microtubules during the formation of cell processes in neuronal and non-neuronal cells. Cell Tissue Res. 1998 Feb;291 (2):163-174
14. National Research Council Committee for the Update of the Guide for the C, Use of Laboratory A. The National Academies Collection: Reports funded by National Institutes of Health. In: Guide for the Care and Use of Laboratory Animals. National Academies Press (US) Copyright © 2011, National Academy of Sciences., Washington (DC).
15. Orikasa M, Matsui K, Oite T, Shimizu F. Massive proteinuria induced in rats by a single intravenous injection of a monoclonal antibody. J Immunol. 1988 Aug;141 (3):807-814
16. Kawachi H, Koike H, Kurihara H, Yaoita E, Orikasa M, et al. Cloning of rat nephrin: expression in developing glomeruli and in proteinuric states. Kidney Int. 2000 May;57 (5):1949-1961.
17. Topham PS, Kawachi H, Haydar SA, Chugh S, Addona TA, Charron KB, et al. Nephritogenic mAb 5-1-6 is directed at the extracellular domain of rat nephrin. J Clin Invest. 1999 Dec;104 (11):1559-1566.
18. Fukusumi Y, Wakamatsu A, Takashima N, Hasegawa E, Miyauchi N, Tomita M, et al. SV2B is essential for the integrity of the glomerular filtration barrier. Lab Invest. 2015 May;95 (5):534-545.
19. Fukusumi Y, Zhang Y, Yamagishi R, Oda K, Watanabe T, Matsui K, et al. Nephrin-Binding Ephrin-B1 at the Slit Diaphragm Controls Podocyte Function through the JNK Pathway. J Am Soc Nephrol. 2018 May;29 (5):1462-1474.
20. Kawachi H, Orikasa M, Matsui K, Iwanaga T, Toyabe S, Oite T, et al. Epitope-specific induction of mesangial lesions with proteinuria by a MoAb against mesangial cell surface antigen. Clin Exp Immunol. 1992 Jan;88 (3):399-404.
21. Han GD, Koike H, Nakatsue T, Suzuki K, Yoneyama H, Narumi S,et al. IFN-inducible protein-10 has a differential role in podocyte during Thy 1.1 glomerulonephritis. J Am Soc Nephrol. 2003 Dec;14 (12):3111-3126.
22. Saleem MA, O'Hare MJ, Reiser J, Coward RJ, Inward CD, Farren T,et al. A conditionally immortalized human podocyte cell line demonstrating nephrin and podocin expression. J Am Soc Nephrol. 2002 Mar;13 (3):630-638.

23. Verderame M, Alcorta D, Egnor M, Smith K, Pollack R. Cytoskeletal F-actin patterns quantitated with fluorescein isothiocyanate-phalloidin in normal and transformed cells. Proc Natl Acad Sci U S A. 1980 Nov;77 (11):6624-6628.
24. Kawachi H, Kurihara H, Topham PS, Brown D, Shia MA, Orikasa M, et al. Slit diaphragm-reactive nephritogenic MAb 5-1-6 alters expression of ZO-1 in rat podocytes. Am J Physiol. 1997 Dec;273 (6 Pt 2):F984-993.
25. Otaki Y, Miyauchi N, Higa M, Takada A, Kuroda T, Gejyo F,et al. Dissociation of NEPH1 from nephrin is involved in development of a rat model of focal segmental glomerulosclerosis. Am J Physiol Renal Physiol. 2008 Nov;295 (5):F1376-1387.
26. Nakatsue T, Koike H, Han GD, Suzuki K, Miyauchi N, Yuan H, et al. Nephrin and podocin dissociate at the onset of proteinuria in experimental membranous nephropathy. Kidney Int. 2005 Jan;67 (6):2239-2253.
27. Lehtonen S, Lehtonen E, Kudlicka K, Holthofer H, Farquhar MG. Nephrin forms a complex with adherens junction proteins and CASK in podocytes and in Madin-Darby canine kidney cells expressing nephrin. Am J Pathol. 2004 Sep;165 (3):923-936.
28. Hsueh YP, Yang FC, Kharazia V, Naisbitt S, Cohen AR, Weinberg RJ,et al. Direct interaction of CASK/LIN-2 and syndecan heparan sulfate proteoglycan and their overlapping distribution in neuronal synapses. J Cell Biol. 1998 Jul;142 (1):139-151.

Figure Legends

Fig. 1 Synbindin is expressed in the slit diaphragm area in podocytes.

(a) IF finding of synbindin in rat kidney section and human cultured podocytes. Clear staining was detected in glomeruli along the capillary loop as a discontinuous dot-like pattern. In human cultured podocytes, a synbindin signal was detected in the cytoplasm and cell membrane area. No positive staining was detected with irrelevant rabbit serum. (Scale bar, 50 μm) (b) Dual-labeling immunofluorescence analysis of synbindin with glomerular cell markers and podocyte subcellular markers. Synbindin staining was clearly apart from endothelial cells marker RECA1 and mesangial cell marker Thy1.1. Synbindin staining was apart from α3-integrin, a basal surface marker of podocyte. Major parts of synbindin were colocalized with slit diaphragm markers nephrin and ephrin-B1. A part of synbindin was colocalized with podocalyxin, an apical surface marker of podocyte (arrow). Scale bar, 20 μm. (c). The developmental expression of synbindin was analyzed by dual-labeling IF study with nephrin. At the early S-shape body stage, no synbindin staining was detected when nephrin expression is not detected yet. At the late S-shape body stage, synbindin appeared together with nephrin. At the capillary loop stage, synbindin staining was colocalized with nephrin. Scale bar, 20 μm.

Fig. 2 Immunostaining of synbindin was lowered in nephrotic models.

Dual-labeling immunofluorescence findings of synbindin with nephrin. (a) In the anti-nephrin antibody-induced nephropathy (ANA), synbindin staining was decreased already at 1 hour, and the alteration became more evident on day 5. The remaining synbindin was apart from the nephrin (arrows). (b) In puromycin aminonucleoside (PAN)-induced nephropathy, synbindin staining was decreased already at 1 hour, and the alteration became evident on day 10. Nephrin remained is colocalized with synbindin. The lower panel showed semiquantitative data. Data are shown as ratios relative to normal findings and expressed as mean ± SEM *P < 0.05 versus normal (*u*-test). n=6 for normal, n=3 in each time point. Scale bar, 20 μm.

Fig. 3 mRNA expressions of synbindin and synbindin-related molecules were decreased in nephrotic models.

mRNA expressions of synbindin and synbindin-related molecules were analyzed in ANA and PAN nephropathies by real-time RT-PCR. Synbindin expression was decreased in both nephropathies. The expressions of syndecan-2, syndecan-4, and CASK were decreased in both models. The data are shown as ratios relative to normal findings and expressed as mean ± SEM of three independent experiments. *P < 0.05, **P < 0.01, ***P

< 0.001 versus normal (*t*-test).

Fig. 4 Synbindin knockdown results in cytoskeletal alteration and downregulation of ephrin-B1 and upregulation of SV2B.

(a) Representative findings of synbindin staining were shown in the left panel, and mRNA expression of synbindin was shown in the right panel. Synbindin downregulation was confirmed by immunofluorescence and real-time RT-PCR *P < 0.05 versus Scramble (*t*-test). Data are shown as mean ± SEM. Scale bar, 50 μm. (b) Representative findings of Rhodamine-phalloidin staining and evaluation of actin staining. Synbindin siRNA-treated cells showed altered cytoskeletal morphology. The F-actin structure was deranged (arrows), and the round-shaped cells without fine processes increased by synbindin siRNA-treatment (arrowheads). Data of semiquantitative analysis were shown in the lower panel. Data are shown as mean ± SEM. **P < 0.01 versus Scramble (*t*-test, Cells forming process: *u*-test, actin score and actin category), Scale bar, 50 μm. (c) mRNA expressions of podocyte functional molecules and synbindin-related molecules in synbindin siRNA treated cells. Downregulation of ephrin-B1 and upregulation of SV2B were detected in synbindin siRNA-treated cells. *P < 0.05 versus Scramble (*t*-test). Data are shown as mean ± SEM.

Figure 1

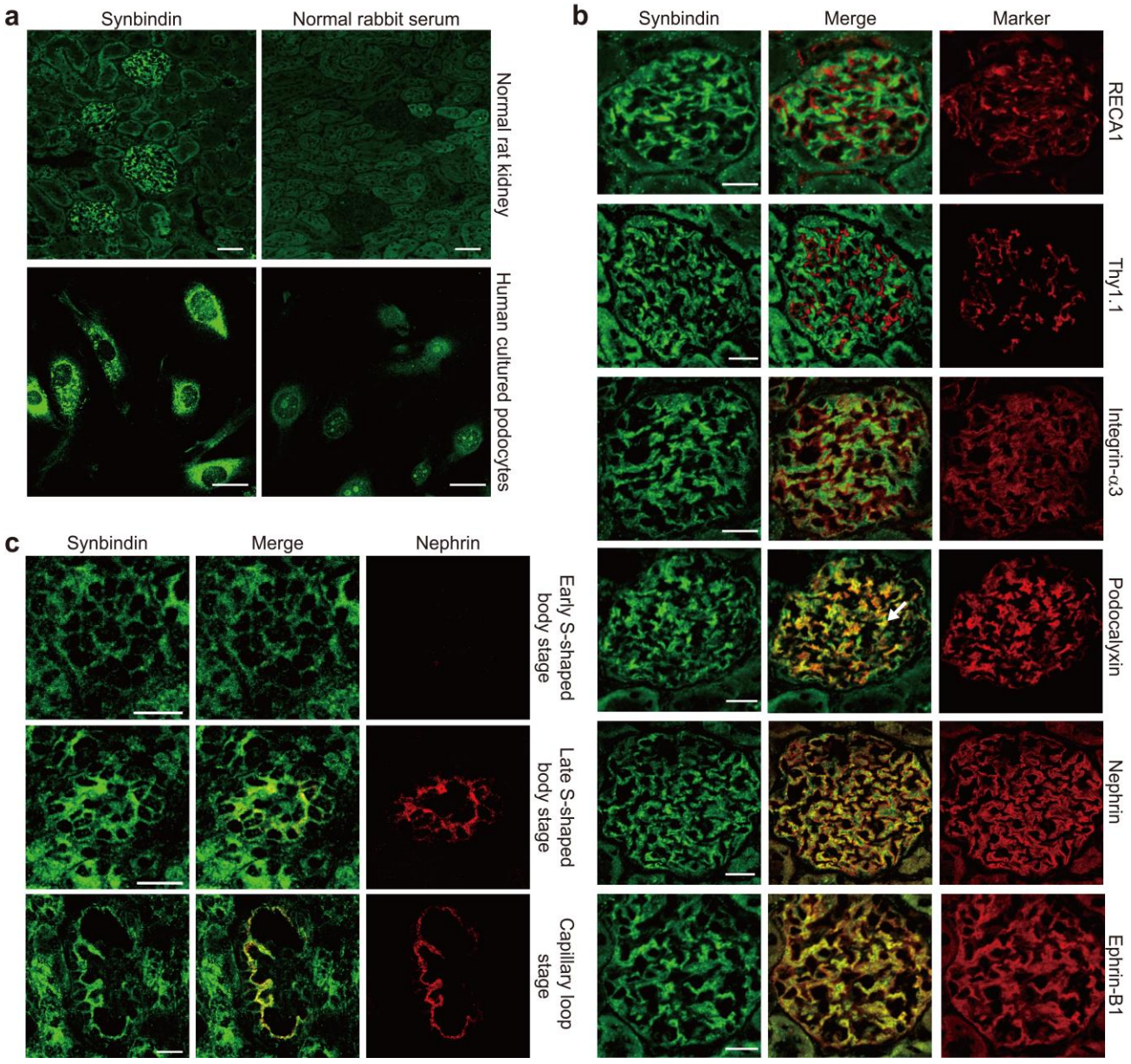
a
Synbindin
Normal rabbit serum
Normal rat kidney
Human cultured podocytes
b
Synbindin
Merge
Marker
RECA1
Thy1.1
Integrin-α3
Podocalyxin
Nephrin
Ephrin-B1
c
Synbindin
Merge
Nephrin
Early S-shaped body stage
Late S-shaped body stage
Capillary loop stage

Figure 2

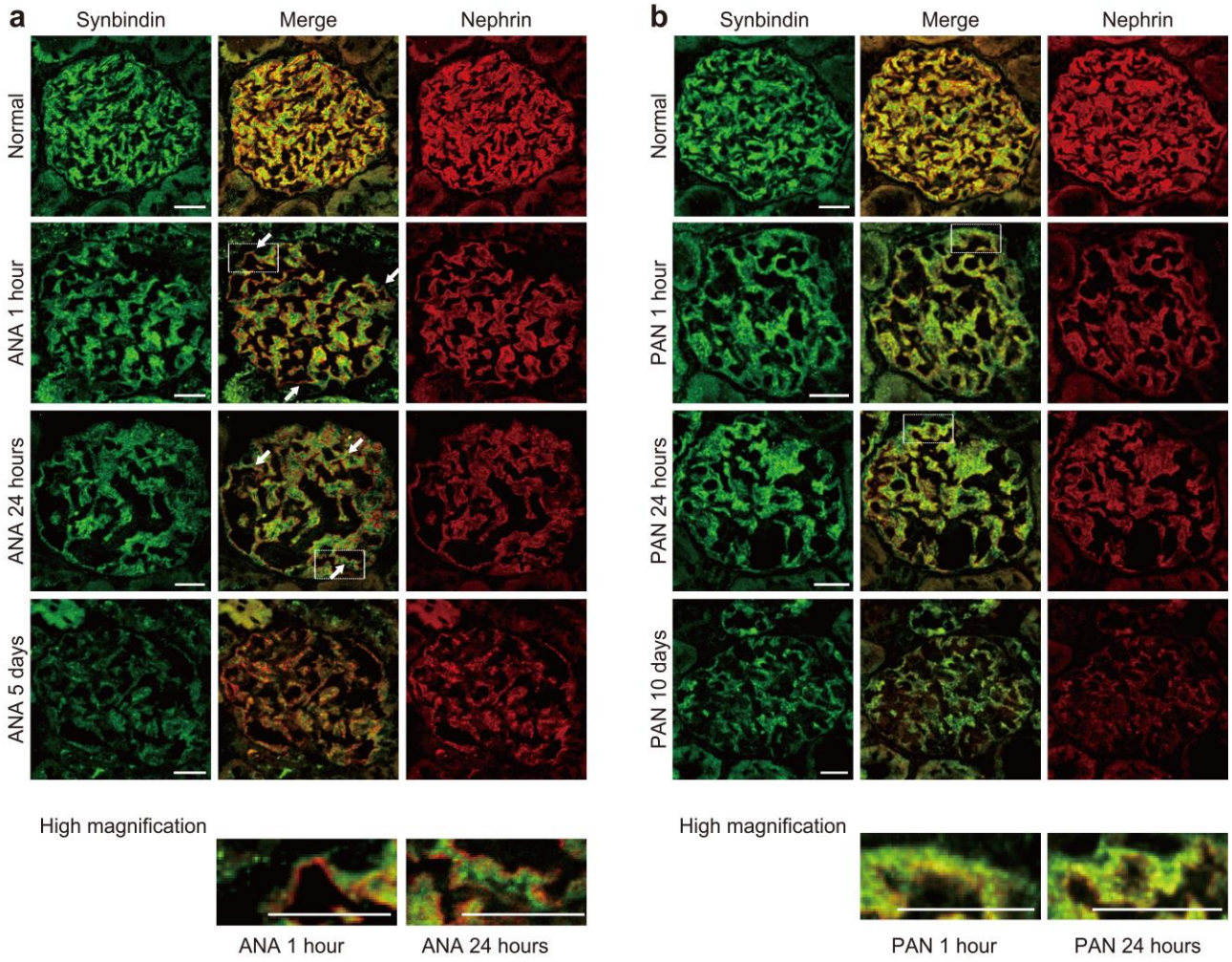
a
Synbindin
Merge
Nephrin
Normal
ANA 1 hour
ANA 24 hours
ANA 5 days
b
Synbindin
Merge
Nephrin
Normal
PAN 1 hour
PAN 24 hours
PAN 10 days
High magnification
ANA 1 hour
ANA 24 hours
High magnification
PAN 1 hour
PAN 24 hours

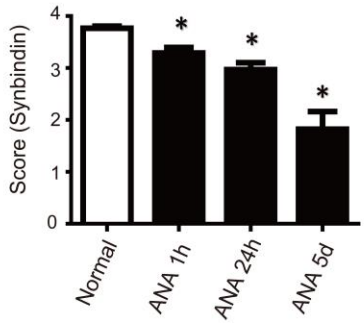
Score (Synbindin)
0
1
2
3
4
*
*
*
Normal
ANA 1h
ANA 24h
ANA 5d

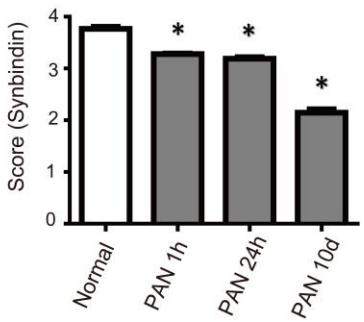
Score (Synbindin)
0
1
2
3
4
*
*
*
Normal
PAN 1h
PAN 24h
PAN 10d

Figure 3

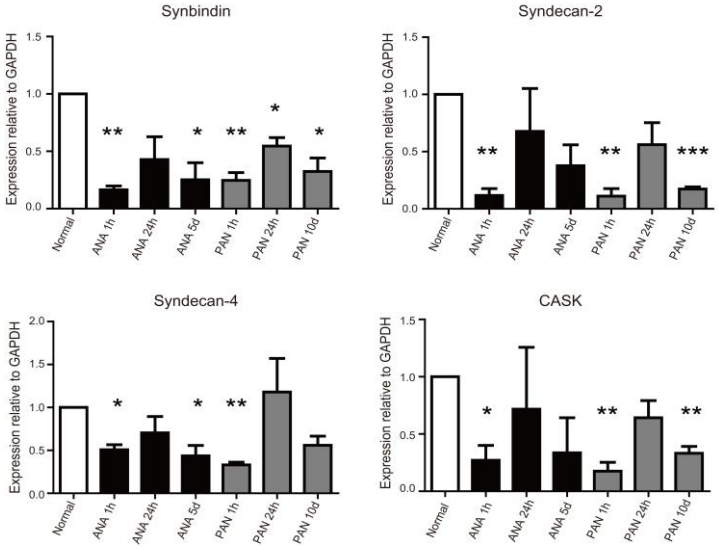
Synbindin
Syndecan-2
Syndecan-4
CASK
Expression relative to GAPDH
Normal
ANA 1h
ANA 24h
ANA 5d
PAN 1h
PAN 24h
PAN 10d

Figure 4

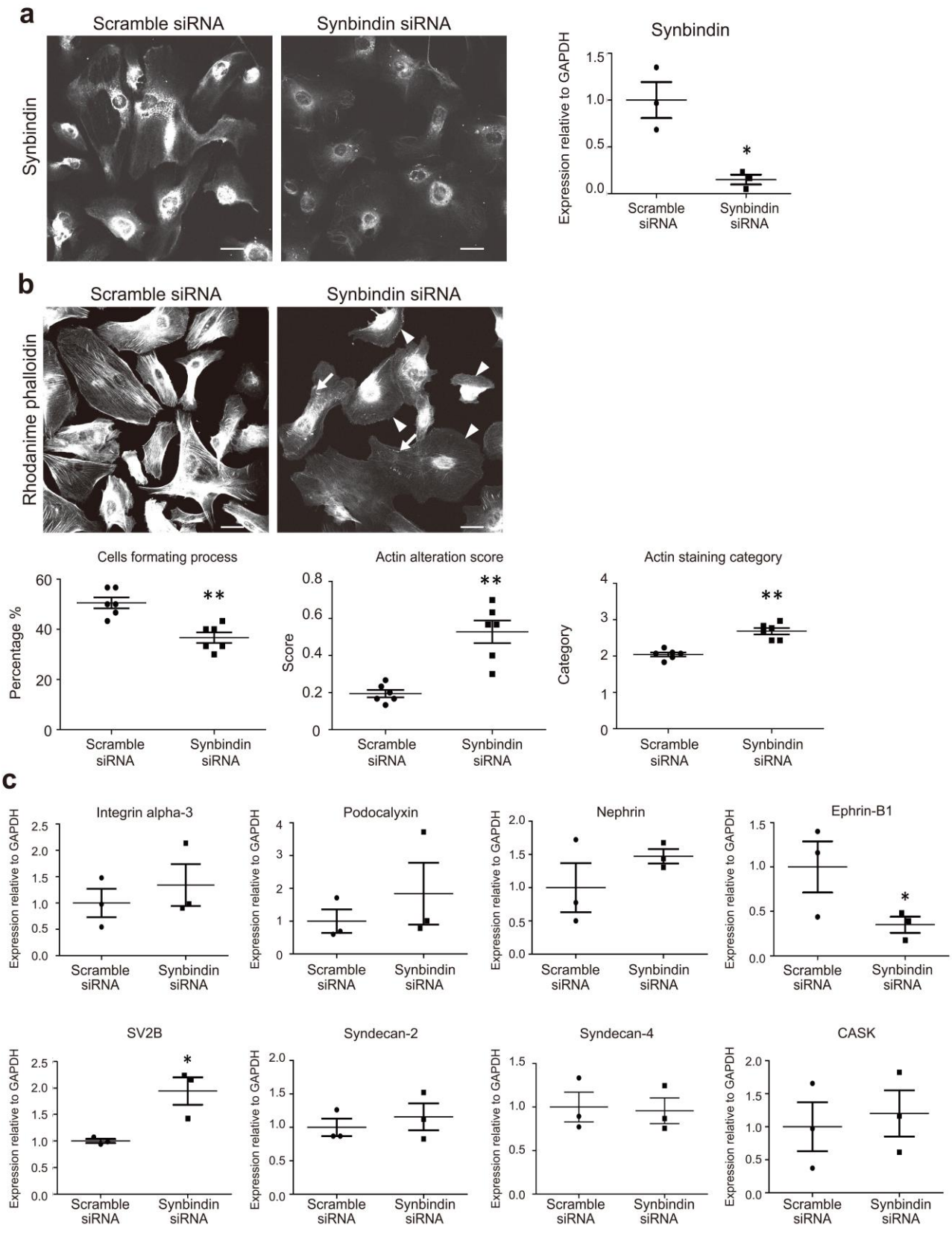
a
Scramble siRNA
Synbindin siRNA
Synbindin
Synbindin
Expression relative to GAPDH
1.5
1.0
0.5
0.0
*
Scramble siRNA
Synbindin siRNA
b
Scramble siRNA
Synbindin siRNA
Rhodanime phalloidin
Cells formating process
Percentage %
60
40
20
0
**
Scramble siRNA
Synbindin siRNA
Actin alteration score
Score
0.8
0.6
0.4
0.2
0
**
Scramble siRNA
Synbindin siRNA
Actin staining category
Category
4
3
2
1
0
**
Scramble siRNA
Synbindin siRNA
c
Integrin alpha-3
Podocalyxin
Nephrin
Ephrin-B1
SV2B
Syndecan-2
Syndecan-4
CASK
Expression relative to GAPDH
Scramble siRNA
Synbindin siRNA
*

Supplementary Information

Synbindin downregulation participates in slit diaphragm dysfunction

Veniamin Ivanov, Yoshiyasu Fukusumi, Ying Zhang, Hidenori Yasuda, Meiko Kitazawa & Hiroshi Kawachi

Department of Cell Biology, Kidney Research Center, Niigata University Graduate School of Medical and Dental Sciences

Correspondence to;

Hiroshi Kawachi, MD, PhD.

Department of Cell Biology, Kidney Research Center, Niigata University Graduate School of Medical and Dental Sciences, Niigata, 951-8510, Japan.

E-mail : kawachi@med.niigata-u.ac.jp.

Phone : +81-25-227-2159, Fax : +81-25-227-0770

Supplemental Table 1. Antibodies used in this study.

Antibodies	References or suppliers	catalog number
mouse anti-RECA1 antibody	Serotec, Oxford, UK	MCA970
mouse anti-Thy1.1 antibody	Ref. 20	
mouse anti-integrin-a3	Santa Cruz Biotechnology, Dallas, TX, USA	sc-7019
mouse anti-podocalyxin antibody	Ref. 21	
mouse anti-nephrin antibody	Ref. 15	
goat anti-ephrin-B1 antibody	R&D Systems, Minneapolis, MN, USA	AF473
FITC-conjugated swine anti-rabbit Igs	DAKO, Glostrup, Denmark	F0205
TRITC-conjugated rabbit anti-mouse Igs	DAKO, Glostrup, Denmark	R0270
TRITC-conjugated rabbit anti-goat IgG	Southern Biotech, Birmingham, AL, USA	6160-03

Supplemental Table 2. Primers used in this study.

Molecule	Primer sequence (5`- 3`)	Product size (bp)	Accession No.
Synbindin (rat)	Sense: CTG GCC TCT ATG TTC CAC TCG C Anti-sence: AGG TTT TGG TCA AAT AGC TC	275	NM_001003708.1
Syndecan-2 (rat)	Sense: ATG CGG GTA CGA GCC ACG TCC Anti-sence: ATA AGC TCC TGA GCC AGA GGC AG	210	NM_013082.4
Syndecan-4 (rat)	Sense: AGG TGA TTT CAC CCT TGG TGC Anti-sence: TGG GTT TCT TGC CCA AGT CG	330	NM_012649.3
CASK (rat)	Sense: AGT GAA GCT GTA GCC AGT CAC Anti-sence: TCC TTG GTT CCG TAG AAA GGC	332	NM_022184.1
Synbindin (human)	Sense: CCA GAC ACT GAC AGG GAT CAA G Anti-sence: CTA TGA CCC AGG TCC AAA AGT TCC	220	NM_016146.6
Syndecan-2 (human)	Sense: GTC TGG CTC GGG AGC TGA TG Anti-sence: AGC AAT GAC AGC TGC TAG GAC	292	NM_002998.4
Syndecan-4 (human)	Sense: TTG TCC ATC CCT TGG TGC CTC Anti-sence: CAT TGG TGG GGG CTT TCT TG	351	NM_002999.4
Podocalyxin (human)	Sense: ACC CAC CGA TAC CCC AAA ACA C Anti-sence: GGC AGG GAG CTT AGT GTG AAT AG	294	NM_001018111.3
CASK (human)	Sense: ATC TAA AGC GGG AAG CCA GTA TC Anti-sence: TGT TCC AAC ACG TCC TCC AG	374	NM_003688.3
Integrin-a3 (human)	Sense: GCA GGC AGA GTT CTG GTC TG Anti-sence: CTT GCG CTG AAT CAT GTA GCT G	291	NM_002204.4
Nephrin (human)	Sense: AGC TCC TTC TAT GGC CTC AAC GTA CTG T Anti-sence: GCG CGG GTC ACA TTC CAC AGA T	233	NM_004646.4
Ephrin-B1 (human)	Sense: AAG AAC CTG GAG CCC GTA TC Anti-sence: GGC TTC CAT TGG ATG TTG AGG	337	NM_004429.5
GAPDH (rat)	Sense: CTC TAC CCA CGG CAA GTT CAA Anti-sence: GGA TGA CCT TGC CCA CAG C	515	NM_017008.4
GAPDH (human)	Sense: TTC CAC CCA TGG CAA ATT CCA Anti-sence: GGA TGA CCT TGC CCA CAG C	515	NM_002046.7